Facile synthesis, characterization of a MnFe$_2$O$_4$/activated carbon magnetic composite and its effectiveness in tetracycline removal

Lina Shao [a,b], Zongming Ren [a], Gaosheng Zhang [a,*], Linlin Chen [a]

[a] Key Laboratory of Coastal Environment Processes, Yantai Institute of Coastal Zone Research, Chinese Academy of Sciences, Yantai 264003, China
[b] School of Environmental and Municipal Engineering, Lanzhou Jiaotong University, Lanzhou 730070, China

ABSTRACT

In this study, MnFe$_2$O$_4$/activated carbon magnetic composites with mass ratio of 1:1, 1:1.5 and 1:2 were synthesized using a simple chemical coprecipitation procedure. A variety of techniques such as X-ray diffractometer, scanning electron microscope, magnetization measurements, BET surface area measurements were used to characterize the structure, morphology and magnetic performance of the prepared composite adsorbents. The results showed that the composites had good magnetic properties, which allowed their convenient magnetic separation from water. Spinel manganese ferrite was found to occur in the magnetic phase and the presence of magnetic particles of MnFe$_2$O$_4$ did not significantly affect the surface area and pore structure of the activated carbon. The magnetic composites were effective for tetracycline (TC) removal from water and the maximal adsorption capacity was 590.5 mmol kg^{-1} at pH 5.0. The TC adsorption followed pseudo-second-order kinetic model and its removal decreases gradually with an increase in pH value, whereas the removal rate was over 60% even at pH 9.0. The TC adsorption process is endothermic and the increase of temperature is favoring its removal. All these results indicated that the prepared composites had the potential to be used as adsorbents for the removal of TC from water or wastewater.

© 2012 Elsevier B.V. All rights reserved.

1. Introduction

As one of the most important antibiotic families, tetracyclines (TCs) are the second most widely used antimicrobial in the world, with applications in human therapy and the livestock industry [1,2]. Most of the TCs (50–80%) used in the farming industry are excreted through feces and urine as unmodified parent compounds, with only small fractions being absorbed in the digestive tract of animals [3,4]. As a result, residues of TCs discharged from municipal wastewater treatment plants (WWTPs) and agricultural runoff are frequently detected in sewage, agricultural wastewater, surface water, groundwater, and even drinking water [5–7]. Exposures to low-level antibiotics in the environment have raised significant concerns of the toxic effect, as well as the transfer and spread of antibiotic resistant genes among microorganisms [7]. As stated by the World Health Organization, the increasing emergence of antibiotic resistance in human pathogens is a special concern, not only for treating infectious disease, but also for other pathologies in which antibiotic prophylaxis is needed for avoiding associated infections [8].

Large molecules of TCs are usually neutral or negatively charged at pH of environmental water. For this reason, the removal of this pharmaceutical reduces by conventional techniques, such as sand filtration, sedimentation, flocculation, coagulation and chlorination [9]. It is thus of great importance to develop efficient and cost-effective treatment technologies for the removal of such compounds.

Adsorption, an effective, economic and simple-operating method, is widely used for the removal of various organic compounds. Various sorbents including natural minerals and synthetic materials such as palygorskite [10], carbon nanotubes [7], montmorillonite, kaolinite [11,12], iron oxides, silica, iron/aluminum hydroxides [13–15] have been employed to remove undesirable TCs from the water. Besides, powdered activated carbon with the properties of high surface area, porous structure and special surface reactivity [16], offers an attractive and inexpensive option for the removal of TCs from water. However, some difficulties are encountered in separating and regenerating spent powdered activated carbon, when the sorbents become exhausted or the effluent reaches the maximum allowable discharge level.

* Corresponding author. Tel.: +86 0535 2109139; fax: +86 0535 2109000.
E-mail addresses: gszhang@yic.ac.cn, zgs77@126.com (G. Zhang).

Such as, filtration, the traditional method for separating powdered activated carbon, could cause the blockage of filters or the loss of carbon; sorbents have been traditionally discarded with the process sludge after use in water and wastewater treatment, resulting in the secondary pollution [17,18].

To overcome the disadvantages of the powdered activated carbon, considerable attention has recently been focused on the fabricating magnetic activated carbon and then separating it using a magnetic separation technology, which is considered as a rapid and effective technique for separating magnetic particles. For examples, Oliveira et al. [19] have synthesized an activated carbon/iron oxide magnetic composites for the adsorption of volatile organic compounds such as chloroform, phenol, chlorobenzene and drimaren red dye from aqueous solution; Zhang et al. [18] have prepared $CuFe_2O_4$/activated carbon to adsorb and catalytically degrade acid orange II; Yang et al. [20] have employed magnetic Fe_3O_4/activated carbon nanocomposite particles for the removal of methylene blue from aqueous solution; Gong et al. [21] have synthesized magnetic multi-wall carbon nanotube nanocomposite as adsorbent for the removal of cationic dyes.

$MnFe_2O_4$, a well known soft magnetic material, has relatively high surface area, saturation magnetization and excellent chemical stability and often regulates free metal and organic matter concentration in soil or water through adsorption reactions [22–24]. Therefore, $MnFe_2O_4$/activated carbon composite combining the advantages of desirable adsorption capacity and effective magnetic separability, could be used as a cost-effective and promising adsorbent to remove a wide range of organic pollutants including TC. However, to our best knowledge, little is known about the preparation of $MnFe_2O_4$/activated carbon composites and their effectiveness in TC removal from water.

The purposes of this research were therefore to prepare $MnFe_2O_4$/activated carbon magnetic composites using a facile coprecipitation method, to characterize the prepared composites with various techniques and then to investigate its effectiveness in TC removal from water, finally to evaluate the feasibility and applicability of using this composite as a potential sorbent to treat wastewater containing higher amounts of TC.

2. Experimental

2.1. Materials

TC was purchased from Beijing Chemical Co. (Beijing, China) and used without further purification. Coconut powdered activated carbon (200 mesh) was produced by Northern Suburb Activated Carbon Plant of Beijing (Beijing, China). All other chemicals, including manganese (II) chloride tetrahydrate, ferric chloride hexahydrate and NaOH obtained from Beijing Chemical Co. (Beijing, China) were analytic grade. All solutions were prepared with deionized water. The chemical structure of the TC is showed as follows:
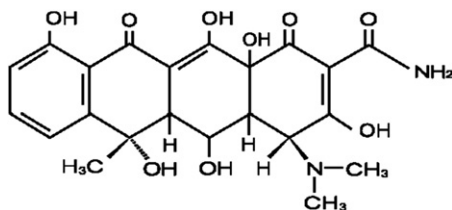
2.2. Preparation of $MnFe_2O_4$/activated carbon magnetic composites

Coprecipitation method was used to prepare $MnFe_2O_4$/activated carbon magnetic composites. In a typical procedure, a certain amount of activated carbon was added into a 200 mL solution which dissolved manganese (II) chloride (0.025 mol) and ferric chloride (0.05 mol) at room temperature. The amount of activated carbon was adjusted to obtain $MnFe_2O_4$/activated carbon mass ratios of 1:1, 1:1.5 and 1:2. Under vigorous stirring, the solution temperature was raised to 3331 K and then 3 mol L^{-1} NaOH solution was added dropwise to the above mixture until the pH value reached 11. Then, another 1 h stirring was continued. Afterwards, the suspension was heated for 4 h at 373 K using a water bath. After cooling, the prepared magnetic composite was repeatedly washed using distilled water to remove the impurities (e.g., Cl^-, Na^+) associated with the procedures. Subsequently, as-prepared composite was separated from water by a simple magnetic procedure, and then was dried in an oven at 383 K.

2.3. Characterization of the composites

The composite was characterized with a VSM model 155 magnetic meter to measure specific saturation magnetization (σs) at room temperature. BET surface area, pore diameter, and pore volume were determined by a surface analyzer (NOVA 4000, Quantachrome Co., USA) with N_2 as the adsorbate. The crystalline structure of $MnFe_2O_4$ in the composite was determined via a D/Max-3A diffractometer (Rigaku Co., Japan) with Cu Kα radiation by the X-ray powder diffraction method. The particle shapes were observed by means of a Hitachi S-3500 N Scanning Electron Microscope (Hitachi Co., Japan) using scanning electron microscopy.

2.4. Batch adsorption experiments

The adsorption kinetics, adsorption isotherm, as well as the influence of initial pH and different temperatures on the adsorption of TC by the $MnFe_2O_4$/activated carbon magnetic composite and activated carbon were determined by batch experiments. For all batch experiments, 50 mg of adsorbent was added to 50 mL of 0.01 mol L^{-1} KCl solution unless otherwise noted. They were combined in 150 mL glass vessels and mixed on an orbital shaker at 120 rpm. The temperature was controlled at a constant temperature 298 ± 1 K. The solution pH adjustment was conducted by adding small amount of 0.1 M HCl and/or 0.1 M NaOH with a pipette.

The adsorption isotherms were generated at pH value of 5.0 ± 0.1 by reacting different amounts of TC (0.1–2 mM) with 50 mg of original activated carbon, $MnFe_2O_4$ and the 1:1.5 composite, respectively. The samples were immediately filtered through a 0.45 μm membrane filter after reaction. The concentrations of TC in the filtered solutions were determined using UV–visible spectroscopy.

For adsorption kinetics, 1.000 g of the composite or activated carbon was added to 1.0 L solution containing 0.5 mM TC and 0.01 M KCl. A constant pH of 5.0 ± 0.1 and temperature of 298 ± 1 K was maintained. Samples were stirred on a stirrer, subsequently, taken at specified time intervals and then filtered through a 0.45 μm membrane filter immediately. The quantity of adsorbed TC was calculated by the difference of the initial and residual amounts of TC in solution divided by the weight of the adsorbent and could be represented by Eq. (1):

$$q_e = \frac{(c_o - c_t)v}{m} \tag{1}$$

where q_e (mmol kg^{-1}) is the sorbed TC at t time, c_o and c_t are the initial and t time concentrations of TC (mmol L^{-1}), respectively, v is the volume of solution (L), and m is the mass of the adsorbent (kg).

In order to study the influence of temperatures on TC adsorption by the 1:1.5 composite, batch tests were carried out at three temperatures of 288, 298 and 308 K at pH 5.0 ± 0.1, respectively. To investigate the effect of pH on TC adsorption, batch experiments were performed between pH 3.0 and 11.0 in one-unit increment. The pH of the solutions was adjusted every 4 h with dilute HCl or/ and NaOH solution to designated values in the range of 3–11 during shaking process. The equilibrium pH was measured and the supernatant was filtered through a 0.45 μm membrane after the solutions were mixed for 24 h.

2.5. Desorption of TC

For the desorption study, 300 mg 1:1.5 composite was introduced into a 500 mL beaker containing 300 mL TC solution (0.5 mmol L^{-1}), and stirred continuously at 120 rpm for 24 h at 298 ± 1 K in order to reach adsorption equilibrium. Upon equilibration, composite was separated by fast filtration. And then, the spent composite was dried at 333 K. The TC concentration of residual solution was determined and the adsorption amount was calculated accordingly.

Subsequently, 50 mg of exhausted composite was transferred into each 150 mL vessel containing 50 mL solution with different concentrations of NaOH (0, 0.001, 0.01, 0.1, and 0.5 M). The solutions were agitated at 120 rpm for 4 h at 298 ± 1 K. The suspension solutions were then filtered and analyzed for TC according to the method described previously. The quantity of desorbed TC was determined by the amount of TC in the solution after the desorption experiment. The TC desorbability was defined as the ratio of the desorbed TC over the total TC adsorbed by the adsorbent.

2.6. Analytical methods

The concentration of TC was analyzed by UV–visible spectroscopy (UV–1810, Puxi Inc., China). The absorbance of TC compound was measured at 360 nm [11]. The pH was measured with a pH meter (Model 720A, Orion Co., USA). The correlation coefficient of the standard curve ($n = 6$) was greater than 0.999. All experiment data in this study were dealt with the software Origin 8.0.

3. Results and discussion

3.1. Characterization of the composites

In order to identify the purity and crystallinity of the samples, XRD analysis was performed on the synthesized MnFe$_2$O$_4$ and the composite samples. As shown in Fig. 1, MnFe$_2$O$_4$ sample yields an XRD pattern that contains diffraction peaks at $2\theta = 18.1°$, $30.2°$, $35.1°$, $43.0°$, $53.5°$, $56.8°$, and $62.5°$, which are well indexed to the crystal plane of spinel ferrite (111), (220), (311), (400), (422), (511), and (440), respectively. All these diffraction peaks in the XRD pattern could be perfectly indexed to the cubic spinel MnFe$_2$O$_4$ (JCPDS card 88–1965). A similar observation was reported in the literatures [25,26]. For the 1:1 composite, except for a new and weak peak at $2\theta = 26.0°$ appeared, showing the presence of small content of Mn$_2$O$_3$ [27,28], the XRD pattern of this composite was almost identical to that of the MnFe$_2$O$_4$ particles. These results showed that the magnetic phase in the MnFe$_2$O$_4$ and composite was cubic spinel MnFe$_2$O$_4$.

The SEM images of activated carbon, the prepared pure manganese ferrite and the 1:1.5 composite were displayed in Fig. 2a–c, respectively. Fig. 2a demonstrated that many pores
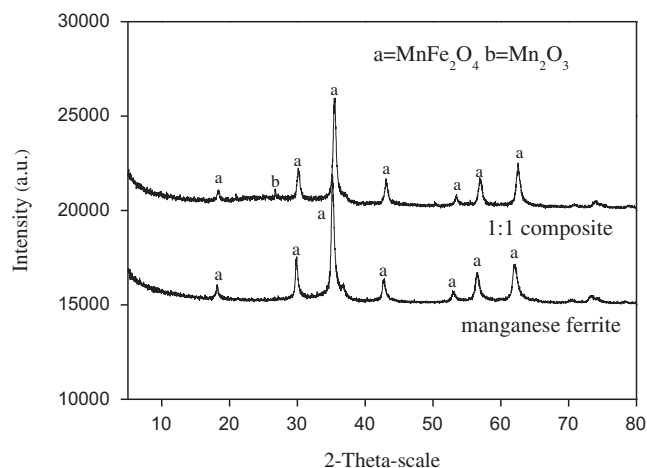

Fig. 1. Powder XRD for the prepared manganese ferrite and the 1:1 MnFe$_2$O$_4$/activated carbon composite.

pervaded homogeneously on the surface of pure activated carbon. As can be seen from Fig. 2b, the agglomeration of many microfine particles led to a rough surface and a porous structure of MnFe$_2$O$_4$. Fig. 2c showed that MnFe$_2$O$_4$ particles with various diameters were distributed on the surface of activated carbon. Although the surface of activated carbon was covered by many small aggregates of manganese ferrite after being incorporated, a porous structure could still be observed, which maintained high adsorbability properties of the activated carbon. The corresponding EDX spectra of the composite was collected and shown in Fig. 2d. The existence of iron, manganese and oxygen on the surface of composite was revealed clearly. This result confirmed further the presence of MnFe$_2$O$_4$ magnetic particles on the surface of activated carbon.

The MnFe$_2$O$_4$ content, magnetization measurement, BET surface area and pore volumes of the pure activated carbon and the prepared composites were listed in Table 1, respectively. Although the surface area and total pore volumes of the composites diminished with an introduction of MnFe$_2$O$_4$ particles, when the percentage of MnFe$_2$O$_4$ in the composite was below 40%, they were not significantly affected by the presence of MnFe$_2$O$_4$ content (e.g. the composites of 1:1.5 and 1:2). The relatively large surface area (512 m^2 g^{-1}) and a high total porous volume (0.46 cm^3 g^{-1}) of 1:1.5 composite, suggested that the pores of the activated carbon were not all blocked by the presence of magnetic MnFe$_2$O$_4$ and the composite was a porous material with good adsorption capacity, which coincided with the SEM observations. However, when the percentage of MnFe$_2$O$_4$ was above 50% (e.g. the composite of 1:1 and pure MnFe$_2$O$_4$), its surface area and total pore volume reduced obviously, compared with those of the pure activated carbon. This may be due to the relatively small surface area of MnFe$_2$O$_4$ that covered partially the activated carbon surface. The similar results have been reported in literatures for the magnetic oxide-supported activated carbon [18,20,29,30].

It can also be observed that the specific saturation magnetization decreased with reducing MnFe$_2$O$_4$ content in the composite. However, this reduce was very sharp, instead of being proportional to the decrease in MnFe$_2$O$_4$ content. Under the preparation conditions employed, two metal oxides could be formed, namely MnFe$_2$O$_4$ and Mn$_2$O$_3$, but only the former is magnetic. The sharp decrease in magnetization of the composite might be attributed to two aspects. One was the increase in non-magnetic Mn$_2$O$_3$ for the composites with higher activated carbon content, which could be confirmed by the XRD analysis. The other was that high carbon content in the composite possibly hindered the crystallization of
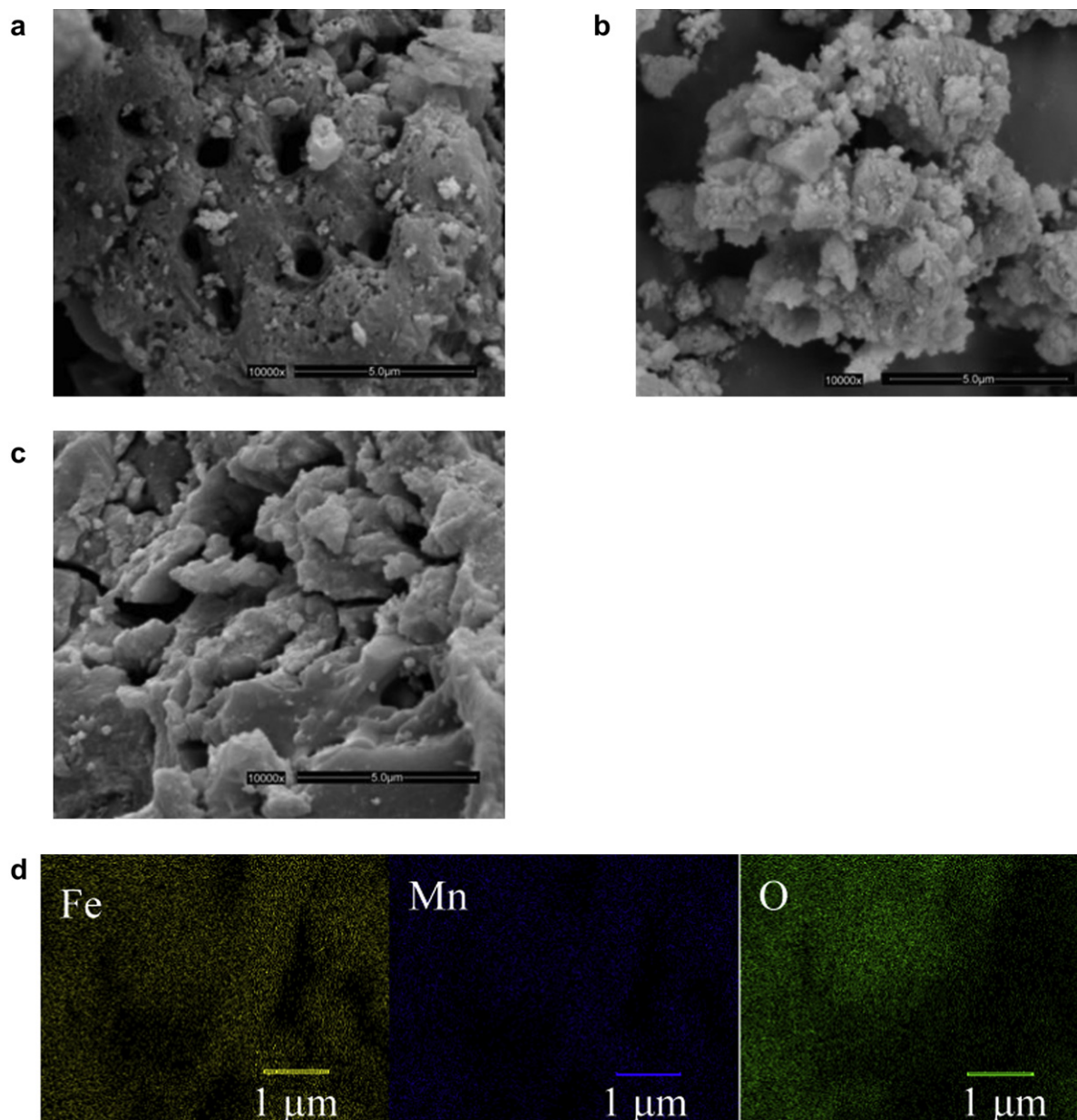
Fig. 2. SEM micrographs of (a) original activated carbon, (b) pure manganese ferrite and (c) 1:1.5 MnFe$_2$O$_4$/activated carbon composite, and (d) EDX mapping of the composite.

MnFe$_2$O$_4$, resulting in smaller particle size of MnFe$_2$O$_4$, which, in turn, lowered its magnetization.

The magnet which magnetic intensity is 0.7 T was placed near the glass bottle to test the magnetic separability of the composite. As displayed in Fig. 3, the water containing dispersed composite was black and turbid. By placing a magnet near the glass bottle, the water changed clear in a short period. The simple experiment proved that composite could be separated easily from solutions with a magnetic separation technique and could be potentially used as a magnetic adsorbent to remove contaminants.

Table 1
Magnetization, BET surface area and pore volume measurements for the MnFe$_2$O$_4$/activated carbon composites.

Composite	MnFe$_2$O$_4$ (wt%)	Specific saturation magnetization (emu g^{-1})	BET surface area (m^2 g^{-1})	Pore volume (cm^3 g^{-1})
Pure activated carbon	0	0	799	0.61
Composite 1:2	33	4.1	553 (750[a])	0.48 (0.6[a])
Composite 1:1.5	40	10.5	512 (748[a])	0.46 (0.61[a])
Composite 1:1	50	22.2	383 (608[a])	0.36 (0.48[a])
MnFe$_2$O$_4$	~100	41.1	158	0.24

[a] Expressed on activated carbon mass basis.

Fig. 3. Magnetic separation of well-dispersed MnFe$_2$O$_4$/activated carbon composite from solution under external magnetic field.

3.2. Adsorption of TC onto the composite

3.2.1. Adsorption isotherm

To evaluate the adsorption capacities of TC on the MnFe$_2$O$_4$ particles, activated carbon and composite, adsorption isotherms were obtained at pH 5.0 using the batch tests and plotted in Fig. 4a. Two-parameter equations (Langmuir and Freundlich equations) were employed to fit the experimental data and constants obtained from the equations were listed in Table 2.

$$\text{Langmuir equation}: q_e = q_{max}\frac{kC_e}{1 + kC_e} \tag{2}$$

$$\text{Freundlich equatio}: q_e = K_F C_e^n \tag{3}$$

where q_e (mmol kg^{-1}) and q_{max} (mmol kg^{-1}) represent the amount of equilibrium adsorption capacity and the maximum adsorption capacity, respectively; C_e (mmol L^{-1}) is the equilibrium solute concentration; k (L mmol^{-1}) is the Langmuir coefficient; K_F is roughly an indicator of the adsorption capacity and n is an empirical parameter.

As seen in Fig. 4a, the adsorption capacity of the composite was a little lower than that of pure activated carbon at low equilibrium TC concentrations (C_e less than 0.5 mmol L^{-1}) while even higher than that of the activated carbon at high equilibrium TC concentrations. The maximal adsorption capacity of q_{max} obtained from the activated carbon and composite were 565.76 mmol kg^{-1} and 590.50 mmol kg^{-1}, respectively. The lower adsorption capacity of the composite at low equilibrium concentrations could be attributed to the fact that the surface area of the activated carbon was reduced after its modification with MnFe$_2$O$_4$ particles. However, the surface was hence more heterogeneous. This might lead to the change of TC adsorption behavior from monolayer adsorption to multilayer adsorption, resulting in increasing adsorption capacity, especially at high equilibrium TC concentrations. As a result, the adsorption capacity of the composite did not change significantly with the decrease in surface area. In addition, complex formation of TC with metal and metal oxide present on the surface of the activated carbon might also contribute to their higher adsorption since compounds with carboxylic and phenolic functional groups are capable of forming complexes with metals [14].

The adsorption capacity of TC on pure the MnFe$_2$O$_4$ was rather lower than the activated carbon, especially at low TC equilibrium
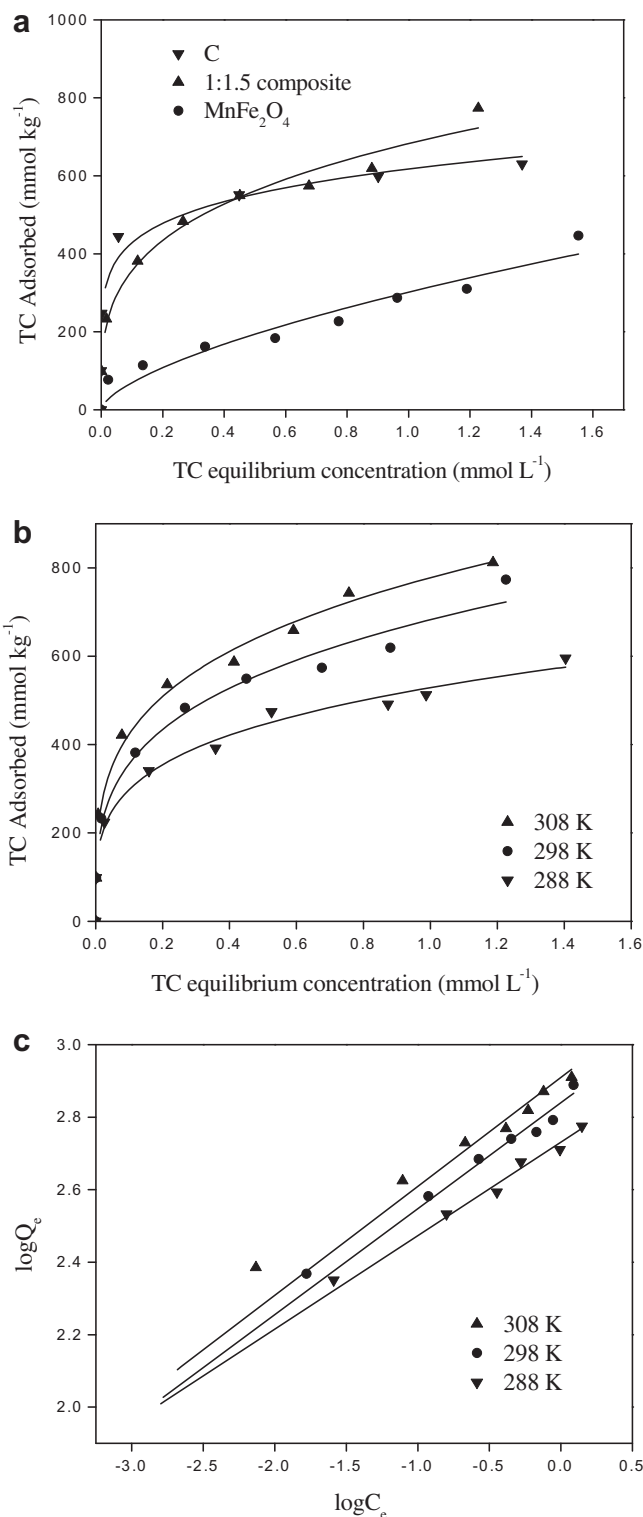

Fig. 4. Adsorption isotherm for TC (a) on original activated carbon, 1:1.5 composite, and MnFe$_2$O$_4$ at pH 5.0 ± 0.1; (b) on 1:1.5 composite at different temperatures, using the Freundlich model; (c) on 1:1.5 composite at different temperatures expressed with the logarithmic form (50 mL TC solution, initial TC concentrations up to 0.5 mmol L^{-1}, pH 5.0 ± 0.1; 25 ± 1 °C; 0.050 g adsorbent).

concentrations. This indicates that the presence of MnFe$_2$O$_4$ in the composite is mainly responsible for the magnetic separability, whereas activated carbon is the main reason for the high adsorption capacity.

Table 2
The isotherms parameters of TC adsorption by activated carbon and MnFe$_2$O$_4$/activated carbon composite at pH 5.0.

Adsorbent	Langmuir model			Freundlich model		
	q_{max} (mmol kg^{-1})	k (L mmol^{-1})	R^2	K_F	n	R^2
Activated carbon	565.76	390.36	0.946	617.62	0.159	0.954
MnFe$_2$O$_4$	106.69	0.400	0.900	301.67	0.638	0.906
MnFe$_2$O$_4$/activated carbon	590.50	27.29	0.911	682.71	0.281	0.978

According to the fitting curves and correlation coefficient values listed in Table 2, TC adsorption onto the 1:1.5 composite was better described by the Freundlich model with a higher correlation coefficient of $R^2 = 0.990$. Due to the heterogeneity of the adsorbent surface with the presence of manganese ferrite, different energies of adsorption sites existed. And the Freundlich equation is generally found to be better suited for describing adsorption where the adsorbent has a heterogeneous surface and adsorption sites with different adsorption energies.

Moreover, the TC adsorption capacity of the composite obtained in this study was compared with those of other adsorbents reported in the literatures on unit mass basis (Table 3). It can be seen that the adsorption capacities of the adsorbents for TC varied markedly. Generally, the value of q_{max} obtained in this study was much higher than that of many other previously reported adsorbents, except for SWNT, indicating that the composite had great potential for application in TC removal from water.

Fig. 4b presented the effect of three different temperatures (288, 298 and 308 K) on TC adsorption at pH 5.0 ± 0.1. Freundlich model was used to fit the experimental data. The values of K_F and n at different temperature were listed in Table 4. It was found that the adsorption capacity increased with increasing temperature, which indicated macroscopically that the adsorption process was endothermic in nature. Therefore, the increase of temperature was favoring the TC removal by this adsorbent.

Fig. 4c demonstrated the results using the logarithmic form of the Freundlich equation.

$$\log q_e = \log K_F + n \log C_e \qquad (4)$$

From this figure, the change of the respective enthalpy ΔH_x of sorption was calculated by the means of the integrated form of the Clausius−Clapeyron equation given by the relation:

$$\Delta H_x = 2.303 R \frac{T_1 T_2}{(T_1 - T_2)} [\log C_{e1} - \log C_{e2}] \qquad (5)$$

For a constant Q_{max} value at three different temperatures ($T_1 = 288$, $T_2 = 298$ and $T_3 = 308$ K) the equilibrium concentrations of solute in the solution at equilibrium (C_{e1}, C_{e2} and C_{e3}) were estimated. ΔH_x was the mean value of three calculations for three pairs of different temperatures and was found to be 26.12 kJ mol^{-1}. The positive value shows an endothermic phenomenon.

The thermodynamic equilibrium constant K_0 for the adsorption process was determined by plotting $\ln q_e / C_e$ versus q_e and extrapolating to zero q_e using a graphical method [31] presented in Fig. 5a. Regression straight lines were fitted through the data points by the least-squares method. The intersection with the vertical axis gives the value of $\ln K_0$ at the three different temperatures.

Additionally, the thermodynamic parameters, such as the changes in free energy (ΔG^0), enthalpy (ΔH^0), and entropy (ΔS^0) can explain the increasing adsorption with increasing temperature. The change in free energy (ΔG^0) was estimated from the known equation, given by the relation:

$$\Delta G^0 = -RT \ln K_0 \qquad (6)$$

where R is the universal gas constant (and T the temperature in K). ΔH^0 and ΔS^0 was estimated according to the van't Hoff equation,

$$\Delta G^0 = \Delta H^0 - T \Delta S^0 \qquad (7)$$

The plot of ΔG^0 versus T was found to be linear (Fig. 5b). Values of ΔS^0 and ΔH^0 were evaluated from the slope and intercept in the diagram. The estimated thermodynamic parameters were presented in Table 5. It was found that the change in Gibbs free energy ΔG^0 was from −25.285 to −29.704 kJ mol^{-1}, the enthalpy change ΔH^0 was = 38.264 kJ mol^{-1}, and the entropy change ΔS^0 was >0 for the sorption. It indicated that the sorption process was spontaneous and endothermic, which accompanied an increase in the degree of freedom.

3.2.2. Effect of pH on TC removal

As shown in Fig. 6, adsorption of TC onto the composite and active carbon was pronounced pH-dependent in the entire pH range studied (3−11). For the activated carbon, the TC removal rate was high under acid and neutral conditions, while gradually decreased with increasing pH and from 95.2% at pH 3.0 to about 64.6% at pH 11.0. A similar trend was also found for the sorption of TC to the composite, which was relatively more obvious when the pH value was above 8.0. However, the TC removal rate was still over 40% at pH around 10 with a high initial TC concentration, indicating that the prepared composite could be used over a broad pH range.

The repulsive force between the functional groups on the surface of activated carbon and TC would be responsible for the

Table 3
Comparison of monolayer adsorption capacities (q_m) of TC on various adsorbents.

Adsorbents	q_m (mmol kg^{-1})	References
MnFe$_2$O$_4$/activated carbon	590.50	This study
Fe/OMC-100	433	[32]
Rectorite	290	[33]
Palygorskite.	210	[10]
Marine sediments	35−69	[34]
Chitosan	93.04	[35]
BDMHDA (benzyldimethylhexadecylammonium)	10[a]	[9]
Montmorillonite	1.66	[12]
Clays	0.056	[11]
Single-walled carbon nanotubes	800−900[a]	[7]
Multi-walled carbon nanotubes	90−100[a]	
Activated carbon	30[a]	
Graphite	70−8.0[a]	

[a] The estimated values according to the isotherms of the literatures.

Table 4
Freundlich isotherm calcuations at different temperatures.

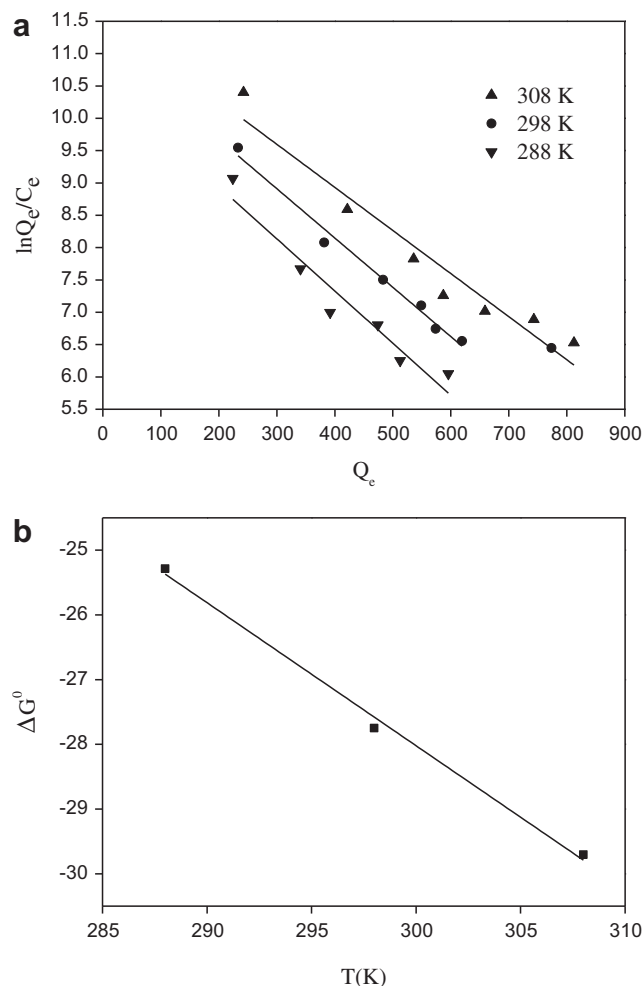|	MnFe$_2$O$_4$/activated carbon + TC		
	R	K_F	n
288 K	0.9668	438.85	0.476
298 K	0.9765	523.23	0.554
308 K	0.9749	579.17	0.558

Fig. 5. (a) Plots of $\ln Q_e/C_e$ versus Q_e for adsorption of TC onto 1:1.5 composite at different temperatures; (b) changes of free energy (thermodynamic calculations).
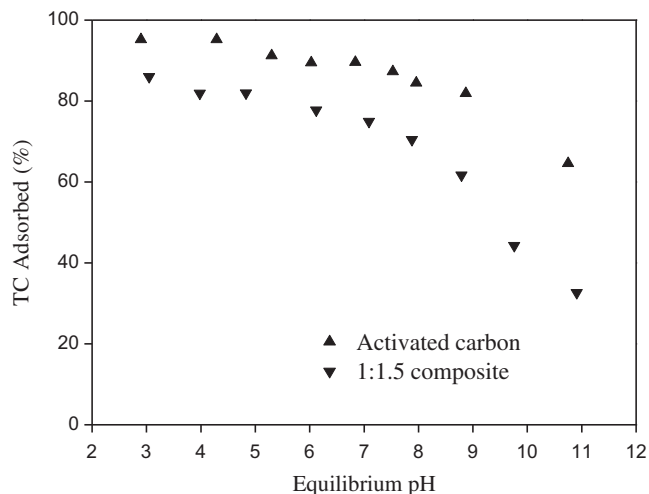

Fig. 6. Effect of solution pH on the adsorption of TC on activated carbon and the 1:1.5 composite (50 mL TC solution, initial concentrations 0.5 mmol L^{-1}, 0.050 g adsorbent).

3.2.3. TC sorption kinetics

In order to assess the rate of TC removal from the water by the activated carbon and the magnetic composite, TC sorption kinetics experiments were performed. The results were plotted in Fig. 7.

The adsorption of TC on the composite was very similar to that of activated carbon, except for slightly lower adsorption amounts. The final concentration of TC for the composite was about 0.012 mM when the initial concentration of TC was 0.5 mM, while the final concentration of TC for the activated carbon was 0.03 mM under the same conditions.

Most of TC uptake rapidly occurred, followed by a relatively slow process. 91.12% of TC adsorption on activated carbon (i.e. 483.09 mmol kg^{-1} of final adsorption) could be obtained within 2 h, which was much faster than TC sorption on rectorite [32] and palygorskite [10]. The fast sorption of TC onto the composite was due to the smaller particle size (about 75 μm) of the adsorbent, which was favorable for the diffusion of TC molecules from solution onto the active sites of the adsorbent. In the subsequent step, the adsorption slowed down because the intraparticle diffusion dominated.
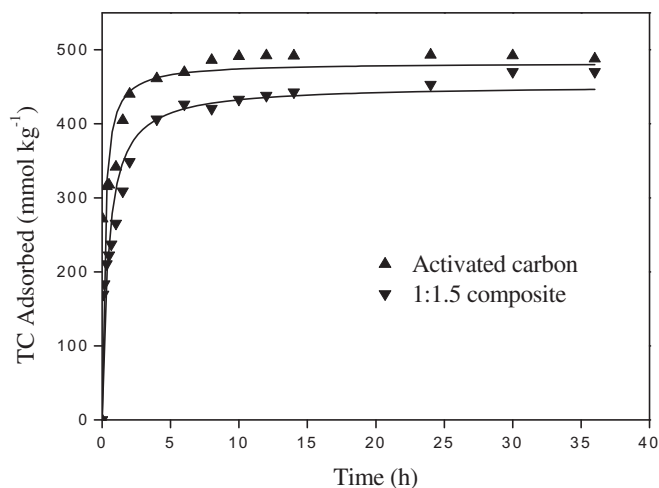
reducing of TC removal at higher pH. TC is an amphoteric compound because of the presence of both Lewis base and Lewis acid functional groups. It may exist predominantly as a cation (+ 0 0) (pH<3.3), when the dimethylammonium group is protonated, as a zwitterion (+ − 0) (3.3 < pH <7.68), resulting from the loss of proton from the phenolic diketone moiety, and as an anion, (+ − −) or (0 − −), due to the loss of protons from the tricarbonyl system and phenolic diketone moiety (pH >7.68) [12]. With the increasing of pH, TC changes from cation in strongly acidic solutions to anionic under alkaline conditions, at the same time, the surface functional groups of activated carbon dissociate, resulting an increase in the negative charge density on the surface. Consequently, the repulsive force between the TC and the surface of the activated carbon or composite increased, and thus reduces the adsorption of TC onto the surface of the adsorbents.

Table 5
Thermodynamic calculations of the sorption process.

T (K)	$\ln K_0$	ΔG^0 (kJ mol^{-1})	ΔH^0 (kJ mol^{-1})	ΔS^0 (J mol^{-1} K^{-1})	ΔH_x (kJ mol^{-1})
288	10.56	−25.285	38.264	220.9	26.12
298	11.20	−27.749			
308	11.60	−29.704			

Fig. 7. Adsorption kinetics of TC on activated carbon and 1:1.5 composite (1000 mL TC solution, initial concentration 0.5 mmol L^{-1}, pH 5.0 ± 0.1; 1.000 g adsorbent).

Table 6
The kinetic model parameters for the adsorption of TC on activated carbon and $MnFe_2O_4$/activated carbon composite at pH 5.0.

Adsorbent	Pseudo-first-order model $q_t = q_e (1 - e^{-kt_1})$			Pseudo-second-order model $q_t = k_2 q_e^2 t/(1 + k_2 q_e t)$		
	q_e (mmol kg^{-1})	K (h^{-1})$_1$	R^2	q_e (mmol kg^{-1})	k_2 (mmol kg^{-1} h^{-1})	R^2
Activated carbon.	470.95	2.41	0.666	483.09	0.0119	0.748
$MnFe_2O_4$/activated carbon	430.50	1.33	0.854	452.49	0.0049	0.929

Langergren pseudo-first-order model and pseudo-second-order model were used to analyze the experimental data (Fig. 7). Kinetic constants obtained for the two models are listed in Table 6. The pseudo-first-order Lagergren equation can be written in the following form:

$$q_t = q_e \left(1 - e^{-k_1 t}\right) \qquad (8)$$

where k_1 is the pseudo-first-order rate constant (h^{-1}), q_e (mmol kg^{-1}) the amount of TC sorbed at equilibrium, and q_t (mmol kg^{-1}) is the amount of TC sorbed on the surface of the sorbent at any time, t.

The integrated rate law of the pseudo-second-order kinetics model [33] is as follows:

$$q_t = \frac{k_2 q_e^2 t}{(1 + k_2 q_e t)} \qquad (9)$$

where k_2 (mmol kg^{-1} h) is the rate constant of the pseudo-second-order adsorption.

It was found that the pseudo-second-order model, used to describe chemisorption, fitted the experimental data better, which was evident from the higher correlation coefficient values (active carbon: $R^2 = 0.748$; composite: $R^2 = 0.929$). It could be concluded that the overall TC adsorption process was controlled by chemical reaction.

3.2.4. Desorption of TC

Desorption of adsorbed TC from the TC-loaded composite was conducted using different concentrations of NaOH solution. The results are presented in Fig. 8. It was clear that the desorption rate of TC increased with an increase in alkalinity and reached a maximal of only 27.6% when the concentration of NaOH was about 0.01 M. Thereafter, d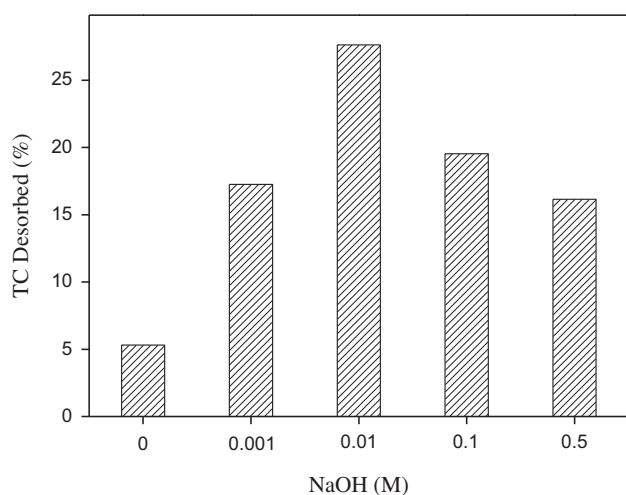esorption rate decreased with further increase in alkalinity. The poor desorption rate revealed that the adsorption of TC on the composite was partially reversible, due to the strong adsorptive interactions between TC and the surfaces of the composite. The phenolic functional groups in TC may be responsible for this strong adsorption because the adsorption of phenolic compounds is found to be strongly influenced by surface functional groups of activated carbon [34]. In a wastewater treatment that uses adsorption, regeneration of the adsorbent is crucially important, and the desorption efficiency directly determines the potential reuse of the adsorbent. Therefore, the efficiency of the composite regeneration will be examined in our next work.

4. Conclusion

In this study, a $MnFe_2O_4$/activated carbon magnetic composite, successfully synthesized using a coprecipitation method was applied to adsorb TC from aqueous solution and exhibited high adsorption efficiency. The presence of the manganese ferrite had no significant decreased in the surface area and in the porosity of the activated carbon, which maintained the high adsorbability of activated carbon. The maximal adsorption capacities of pure activated carbon and the composite were 565.76 mmol kg^{-1} and 590.50 mmol kg^{-1} at pH 5.0, respectively. The TC adsorption process on the composite is endothermic in nature and the increase of temperature is favoring its adsorption. The low solution pH favored the TC adsorption. Additionally, the process of adsorption was relatively rapid, and over 91.12% of the equilibrium adsorption capacity was achieved within 2 h. Adsorbed TC could not be effectively desorbed by NaOH solution. The magnetic composite could be easily separated from solution using a magnetic technique and the composite could be used as a promising and effective adsorbent for the removal of TC from aqueous solutions.

Fig. 8. Desorption of TC from 1:1.5 composite using different concentrations of NaOH solution (exhausted adsorbent dose 1 g L^{-1}, equilibrium time 4 h, temperature 25 ± 1 °C).

References

[1] N.F. Col, R.W. O'Connor, Rev. Infect. Dis. 9 (1987) 232.
[2] S. Kim, P. Eichhorn, J.N. Jensen, A.S. Weber, D.S. Aga, Environ. Sci. Technol. 39 (2005) 5816.
[3] B.S. Halling, Chemosphere 40 (2000) 731.
[4] A.K. Sarmah, M.T. Meyer, A.B.A. Boxall, Chemosphere 65 (2006) 725.
[5] R. Hirsch, T. Ternes, K. Haberer, K.L. Kratz, Sci. Total Environ. 225 (1999) 109.
[6] K.J. Choi, S.G. Kim, C.W. Kim, S.H. Kim, Chemosphere 66 (2007) 977.
[7] L.L. Ji, W. Chen, L. Duan, D.Q. Zhu, Environ. Sci. Technol. 43 (2009) 2322.
[8] J.L. Martinez, Environ. Pollut. 157 (2009) 2893.
[9] T. Polubesova, D. Zadaka, L. Groisman, S. Nir, Water Res. 40 (2006) 2369.
[10] P.H. Chang, Z.H. Li, T.L. Yu, S. Munkhbayer, T.H. Kuo, Y.C. Hung, J.S. Jean, K.H. Lin, J. Hazard. Mater. 165 (2009) 148.
[11] R.A. Figueroa, A. Leonard, A.A. MacKay, Environ. Sci. Technol. 38 (2004) 476.
[12] P. Kulshrestha, R.F. Giese Jr., D.S. Aga, Environ. Sci. Technol. 38 (2004) 4097.
[13] R.A. Figueroa, A.A. MacKay, Environ. Sci. Technol. 39 (2005) 6664.
[14] C. Gu, K.G. Karthikeyan, Environ. Sci. Technol. 39 (2005) 2660.
[15] I. Turku, T. Sainio, E. Paatero, Environ. Chem. Lett. 5 (2007) 225.

[16] K. Gadkaree, Carbon 36 (1998) 981.
[17] D. Clifford, P. Chu, A. Lau, Water Res. 17 (1983) 1125.
[18] G.S. Zhang, J.H. Qu, H.J. Liu, A.T. Cooper, R.C. Wu, Chemosphere 68 (2007) 1058.
[19] L.C.A. Oliveira, R.V.R.A. Rios, J.D. Fabris, V.K. Garg, K. Sapag, R.M. Lago, Carbon 40 (2002) 2177.
[20] N. Yang, S.M. Zhu, D. Zhang, S. Xu, Mater. Lett. 62 (2008) 645.
[21] J.L. Gong, B. Wang, G.M. Zeng, C.P. Yang, C.G. Niu, Q.Y. Niu, W.J. Zhou, Y. Liang, J. Hazard. Mater. 164 (2009) 1517.
[22] C.A. Backes, R.G. McLaren, A.W. Rate, R.S. Swift, Soil Sci. Soc. Am. J. 59 (1995) 778.
[23] M. Muroi, R. Street, P.G. McCormick, J. Amighian, Phys. Rev. B 63 (2001) 184414.
[24] R.C. Wu, J.H. Qu, J. Chem. Technol. Biotechnol. 80 (2005) 20.
[25] H.M. Xiao, X.M. Liu, Y.F. Shao, Compos. Sci. Technol. 66 (2006) 2003.

[26] L. Zhen, K. He, C.Y. Xu, W.Z. Shao, J. Magn. Magn. Mater. 320 (2008) 2672.
[27] M.N. Salavati, F. Mohandes, F. Davar, K. Saberyan, Appl. Surf. Sci. 256 (2009) 1476.
[28] J. Hu, I.M.C. Lo, G.H. Chen, Langmuir 21 (2005) 11173.
[29] C.S. Castro, M.C. Guerreiro, M. Goncalves, L.C.A. Oliveira, A.S. Anastácio, J. Hazard. Mater. 164 (2009) 609.
[30] L.H. Ai, H.Y. Huang, Z.L. Chen, X. Wei, J. Jiang, Chem. Eng. J. 156 (2010) 243.
[31] X. Yuan, W. Xing, S.P. Zhuo, Z.H. Han, G.Q. Wang, X.L. Gao, Z.F. Yan, Microporous Mesoporous Mater. 117 (2009) 678.
[32] P.H. Chang, Z. Li, W.T. Jiang, J.S. Jean, Colloids Surf. A Physicochem. Eng. Asp. 339 (2009) 94.
[33] X.R. Xu, X.Y. Li, Chemosphere 78 (2010) 430.
[34] J. Kang, H.J. Liu, Y.M. Zheng, J.H. Qu, J.P. Chen, J. Colloid Interface Sci. 344 (2009) 117.
[35] M.R. Unnithan, T.S. Anirudhan, Ind. Eng. Chem. Res. 40 (2001) 2693.